

1 **Novel Treatment of Chronic Graft-Versus-Host Disease in Mice Using the ER**
2 **Stress Reducer 4-Phenylbutyric Acid**

3 Shin Mukai,^{1, 3} Yoko Ogawa,¹ Fumihiko Urano,² Chie Kudo-Saito,³ Yutaka Kawakami,³
4 Kazuo Tsubota¹

5

6 ¹Department of Ophthalmology, Keio University School of Medicine, ²Department of
7 Medicine, Division of Endocrinology, Metabolism, and Lipid Research, and Department of
8 Pathology and Immunology, Washington University School of Medicine, ³Institute for
9 Advanced Medical Research, Keio University School of Medicine.

10

11 **This study was supported by the Japanese Ministry of Education, Science, Sports and**
12 **Culture, #26462668**

13

14

15

16

17

18

19

20

21

22

23

24

25 **Supplementary Methods**

26 **Histological analysis and immunohistochemistry**

27 Three or four weeks after BMT, extra-orbital lacrimal glands, the proximal part of small
28 intestine, dorsum skin, liver, salivary glands, lung, large intestine and eyes were collected
29 from the transplant recipients. These samples were subsequently fixed with 10% neutral-
30 buffered formalin and embedded in paraffin. The paraffin blocks were cut into 7µm-thick
31 sections, and then stained with (1) hematoxylin and eosin, (2) Mallory's trichrome^{1, 2} and (3)
32 antibodies used in this study. For immunohistochemical assays, paraffin was removed in the
33 first instance, followed by the recovery of the antigens using either of the following 2 antigen
34 retrieval methods. (A) To stain the sections with a CD45 antibody (30-F11, BD Pharmingen,
35 San Jose, CA), they were immersed in the antigen retrieval solution (Target Retrieval
36 Solution; Dako, Glostrup, Denmark) and then boiled with a microwave oven for 10 min. (B)
37 In the case of multiple staining for CD68 (FA-11, AbD Serotec, Kidlington, UK) and CHOP
38 (F-168, Santa Cruz Biotechnology, Santa Cruz, CA), the sections were soaked in the antigen
39 retrieval solution (HistoVT One; Nakalai Tesque, Kyoto, Japan) and subsequently heated at
40 90 °C for 40 min with a water bath. Next, the sections were blocked with 10% normal goat
41 serum, and the reactions between the antigens in tissue sections and the primary antibodies
42 were conducted at 4°C overnight. The sections were then treated with fluorophore-labelled
43 secondary antibodies at RT for 45 minutes and mounted with an anti-fading mounting
44 medium (Fluorescent Mounting Medium; Dako). Fluorescence images were taken with an
45 LSM confocal microscope (Carl Zeiss, Jena, Germany). As for the counting of CD45⁺ cells,
46 five areas of each tissue section were randomly photographed under 200X magnification, and
47 the number of CD45⁺ cells in the individual images was subsequently determined.

48 The following secondary antibodies were used in this study: goat anti-mouse IgG (H+L)
49 secondary antibody, Alexa Fluor 488 conjugate (Molecular Probes, Eugene, OR) and goat
50 anti-rat IgG (H+L) secondary antibody, Alexa Fluor 568 conjugate (Molecular Probes). With
51 respect to isotype controls, rat IgG2b, κ (eB149/10H5, eBioscience, San Diego, CA), rat
52 IgG2a (54447, R&D Systems, Minneapolis, MN) and rabbit IgG (Cell Signaling Technology,
53 Danvers, MA) were utilized for CD45, CD68 and CHOP, respectively.

54 **Electron microscopy**

55 Transmission electron microscopic analysis was performed according to standard protocols.
56 Tissues were collected from the murine lacrimal glands and small intestine, immediately
57 fixed with 2.5% glutaraldehyde in 0.1 M phosphate buffer (pH 7.4) at 4°C for 4 hours and
58 washed three times with 0.1 M phosphate buffer. The samples were subsequently fixed again
59 with 2% osmium tetroxide, dehydrated in a graded series of ethanol and 100% propylene
60 oxide, and embedded in epoxy resin. One micrometer sections were made from the processed
61 tissues and then stained with methylene blue. The thick sections were observed with a
62 microscope to find parts which were suitable for preparation of ultrathin sections. The
63 obtained sections were placed on mesh grids, stained with uranylacetate and lead citrate, and
64 examined with an electron microscope (1230 EXII; JOEL, Tokyo, Japan). All electron
65 micrographs were acquired with a bio scan camera (Gatan bio scan camera model 792, Tokyo,
66 Japan).

67 **Immunoblotting analysis**

68 The tissues of interest were placed in Eppendorf tubes, and pre-cooled RIPA buffer was
69 added to the tubes. The tissues were then homogenized using an electric homogenizer. After
70 the samples were on ice for 1h, they were centrifuged at 15000 rpm at 4°C for 5 min. The
71 supernatants were subsequently collected in fresh tubes on ice and used as cell lysates. An

72 equal amount of 5X Laemmli buffer was added to each cell lysate, followed by protein
73 denaturation at 100°C for 5 min. Equal amounts of protein from each sample were loaded
74 into the wells of SDS-PAGE gels and then resolved. The proteins were transferred from the
75 gels to membranes at 15 V for 20 min. The membranes were blocked with 5% skim milk or
76 5% BSA in 1 x TBST (a mixture of tris-buffered saline and tween 20) at RT for 1h. The
77 membranes were then incubated with primary antibodies at 4°C overnight. The primary
78 antibodies were diluted 1000 times with 5% skim milk or 5% BSA in 1 x TBST. After the
79 primary antibody incubation, the membranes were washed with 1 x TBST (3 x 10 min),
80 subjected to secondary antibody at RT for 1h and then washed with 1 x TBST (3 x 10 min)
81 and 1 x TBS (2 x 10 min). The proteins of interest were visualized using either of the
82 following two methods. (1) Colorimetric detection of the target proteins was conducted using
83 BCIP/NBT substrate (Promega, WI). (2) Signals were developed with an enhanced
84 chemoluminescence (ECL) detection reagent (GE Healthcare, Littlecalfont, UK), and the
85 target proteins were subsequently visualized with a LAS 4000 mini chemiluminescence
86 imaging system (Fujifilm/GE Healthcare). Densitometric analysis of the obtained protein
87 bands was conducted by the use of the image processing software ImageJ. The primary
88 antibodies used in this experiment were as follows: GRP78 (Abcam, Cambridge, UK),
89 phospho-PERK (Thr980, Cell Signaling Technology), PERK (C33E10, Cell Signaling
90 Technology), phospho-IRE1 α (Thermo Fisher Scientific, Waltham, MA), IRE1 α (14C10
91 Cell Signaling Technology), phospho-eIF2 α (119A11, Cell Signaling Technology), eIF2 α
92 (Cell Signaling Technology), CHOP (9C8, Thermo Fisher Scientific), TXNIP (D5F3E, Cell
93 Signaling Technology) NF- κ B (Abcam), HSP47 (SPA-470, Stress Gen Biotechnologies Corp,
94 San Diego, CA), CTGF (Abcam), α -SMA (1A4, Abcam), CD68 (FA-11, Abcam),
95 Cytokeratin (C-11, Abcam), CD3 (Abcam), CD19 (Cell Signaling Technology), CD20 (D-10,

96 Santa Cruz) and β -actin (AC-15, Abcam). With regards to the secondary antibodies, (1) when
97 the protein bands were visualized by developing a color, either an AP-conjugated anti-mouse
98 IgG antibody (Promega), an AP-conjugated anti-rabbit IgG antibody (Promega) or AP-
99 conjugated anti-rat IgG antibody (Promega) was used, and (2) either an HRP-conjugated anti-
100 mouse antibody (Thermo Fisher Scientific) or an HRP-conjugated anti-rabbit antibody
101 (Thermo Fisher Scientific) was required to detect the target proteins by ECL.

102 **Enzyme linked immunosorbent assay (ELISA)**

103 Blood was collected from PBA- and vehicle-medicated mice and subsequently centrifuged at
104 4000 rpm for 10 min. The levels of MCP-1, tumor necrosis factor- α (TNF- α), and interferon-
105 γ (IFN- γ) in the obtained sera were measured utilizing ELISA sets (Becton Dickinson). These
106 assays were conducted according to the protocols provided by the manufacturer Becton
107 Dickinson.

108

109

110

111

112

113

114

115

116

117

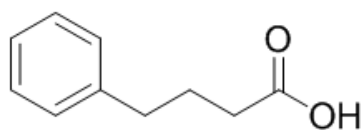
118

119

120 **Supplementary figures**

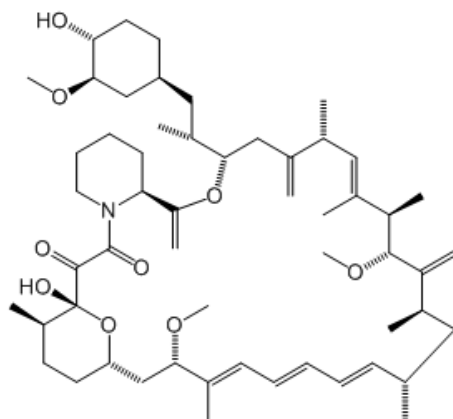
Supplementary Figure 1

A



4-Phenylbutyric acid (PBA)

B



Rapamycin

121

122 **Supplementary Figure 1. Structures of the ER stress reducers (A) 4-phenylbutyric acid**
123 **(PBA) and (B) rapamycin**

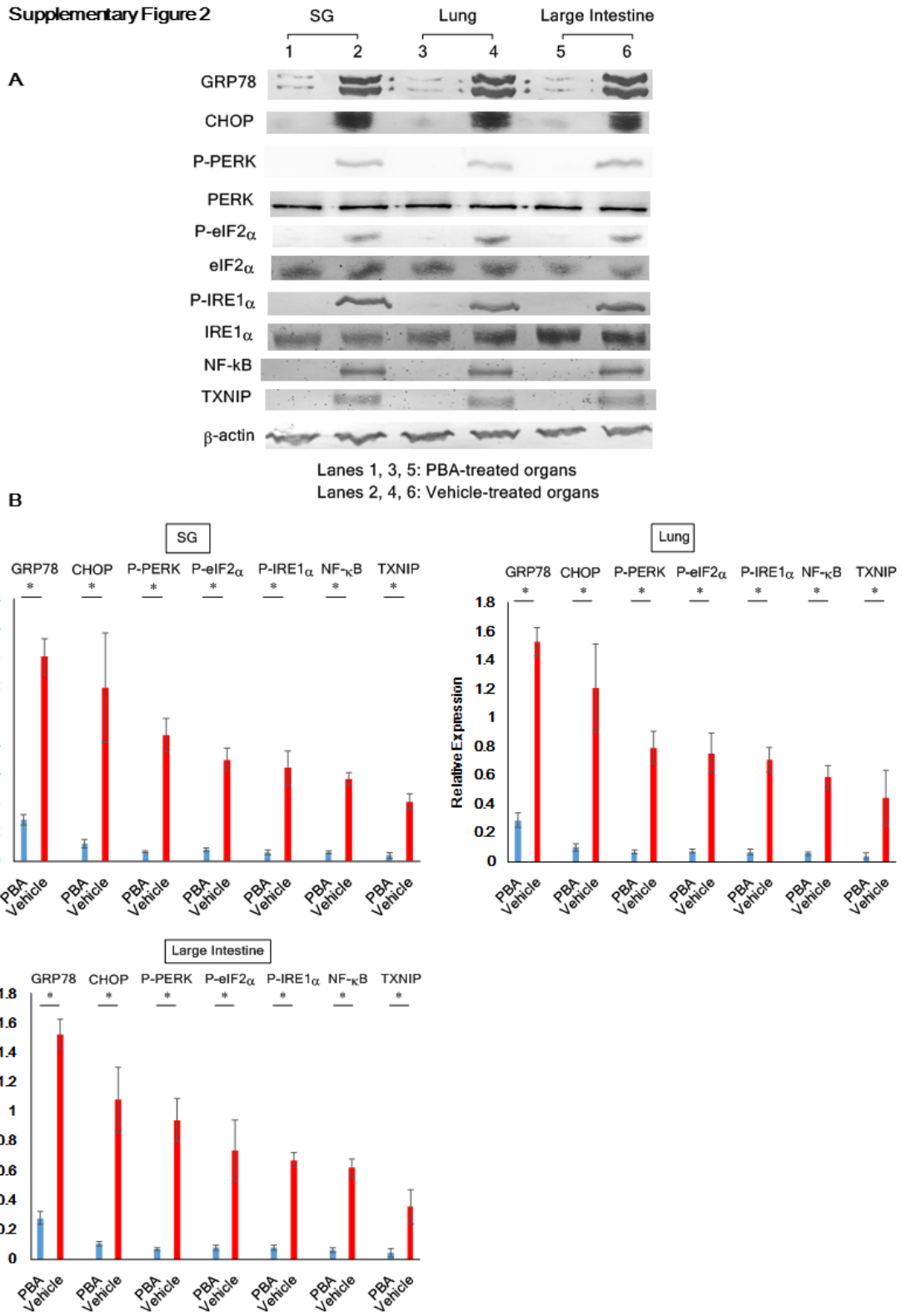
124

125

126

127

Supplementary Figure 2



128
129
130
131

132 **Supplementary Figure 2. Suppression of cGVHD-caused ER stress by PBA.** (A)
133 Immunoblot assays of ER stress markers and the associated inflammatory molecules in
134 cGVHD target organs. (Lanes 1, 3, 5: PBA-medicated organs. Lanes 2, 4, 6: Vehicle-
135 medicated organs) Cropped blots are displayed. (B) The target proteins in each organ were
136 subsequently quantified by densitometry. PBA-treated organs (blue) and vehicle-treated
137 organs (red). Data from one of two similar experiments are shown. The data are presented as
138 means, \pm SD, PBA: n=4, Vehicle: n=4 *P<0.05.

139

140

141

142

143

144

145

146

147

148

149

150

151

152

153

154

155

156

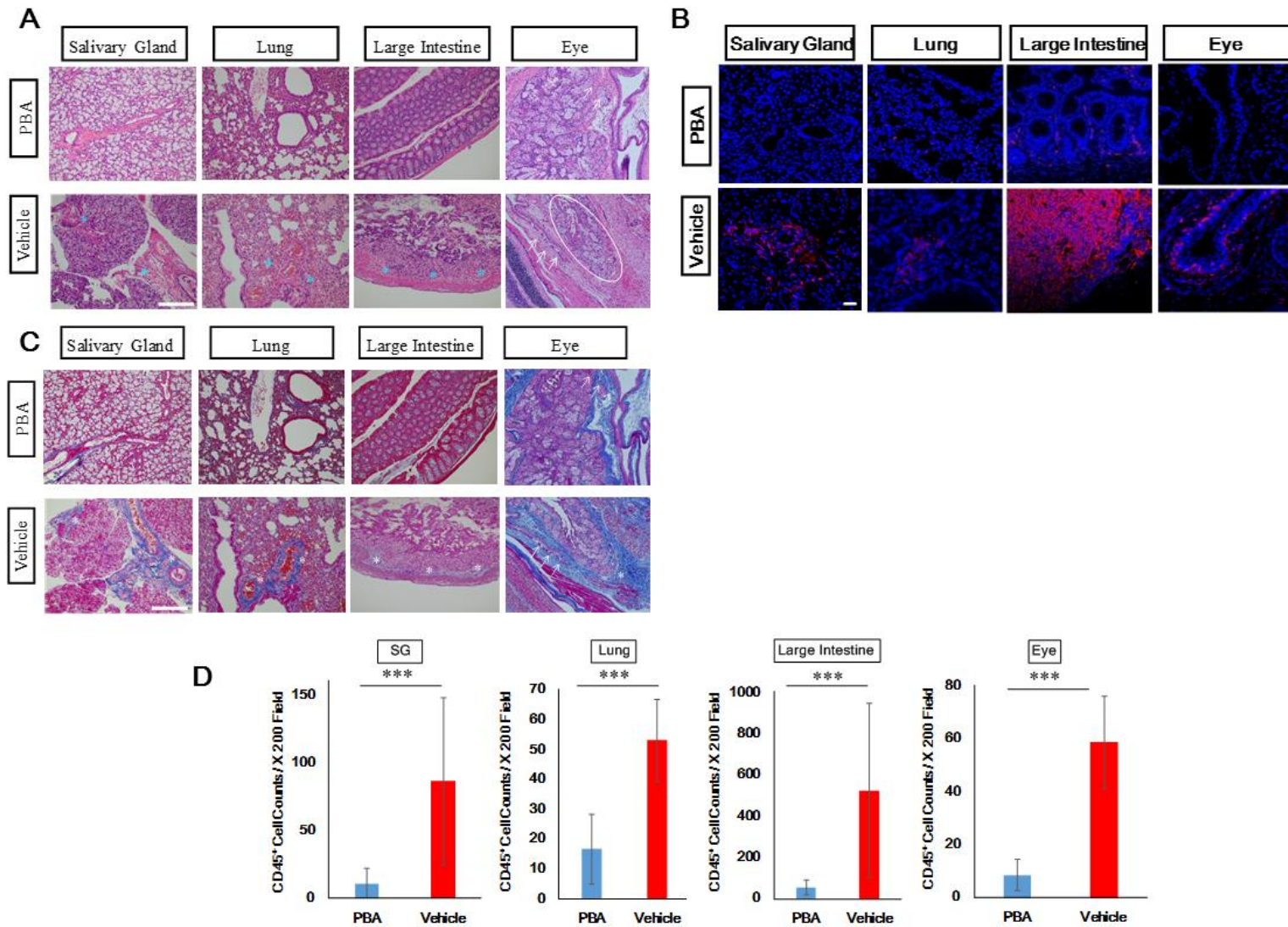
157

158

159

160

Supplementary Figure 3



162 **Supplementary Figure 3. Mitigation of cGVHD-elicited systemic inflammation and**
163 **fibrosis using the ER stress mitigator PBA.** (A) HE pictures of the PBA-treated organs and
164 those treated with the solvent-vehicle. The images were taken at 200x magnification, and the
165 scale bar is 200 μm . Severely inflamed portions are shown with asterisks. In the pictures of
166 the vehicle-medicated eye, an ellipse is placed where its meibomian glands were decreased
167 and shrunk, and conjunctival epithelia are indicated with arrows. (B) Immunostaining for the
168 generic leukocyte marker CD45 in the PBA-medicated tissues and their vehicle-medicated
169 equivalents. CD45⁺ cells and cell nuclei were stained red and blue, respectively. The images
170 were taken at 200x magnification, and the scale bar is 20 μm . (C) Mallory's staining for the
171 PBA-injected organs and their vehicle-injected counterparts. The photographs were taken at
172 200x magnification, and the scale bar is 200 μm . Aberrantly fibrotic areas are shown with
173 white asterisks. (D) The density of CD45⁺ cells in the PBA-treated and their vehicle-treated
174 counterparts. PBA-treated organs (blue) and vehicle-treated organs (red). Data from one of
175 two similar experiments are shown. The data are presented as means, \pm SD, PBA n=3,
176 Vehicle: n=3, *P<0.05, **P<0.01, ***P<0.001.

177

178

179

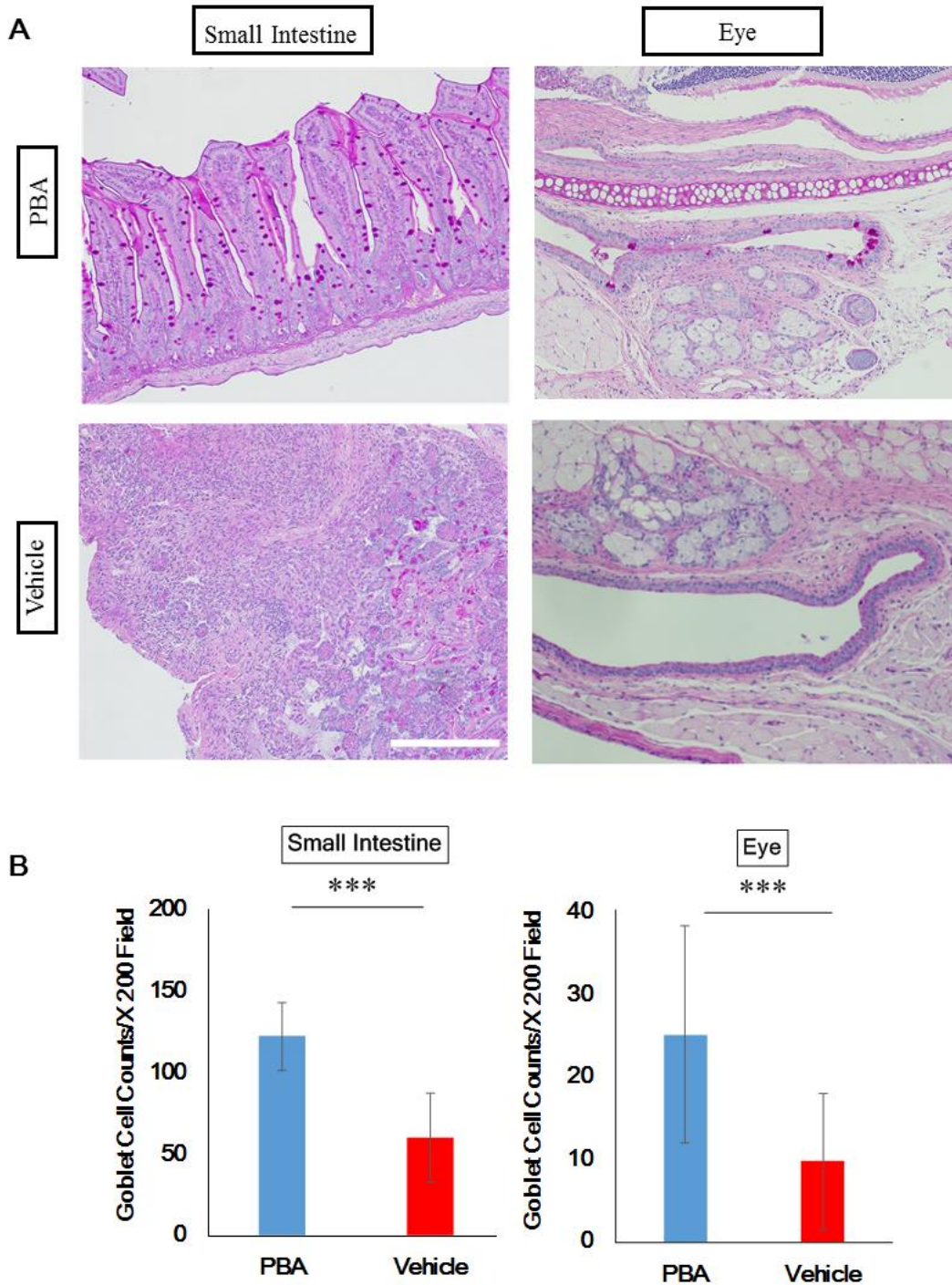
180

181

182

183

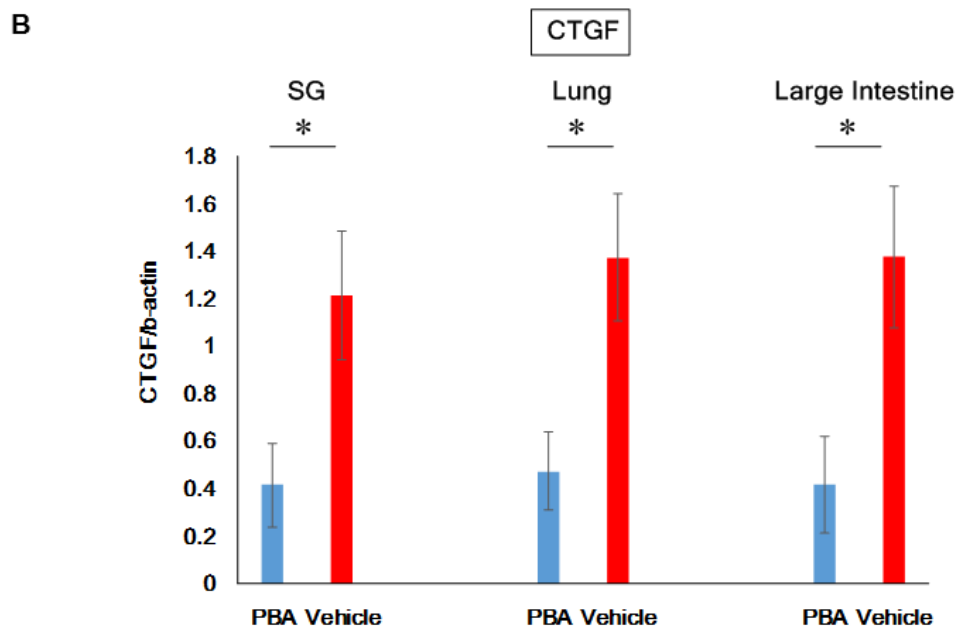
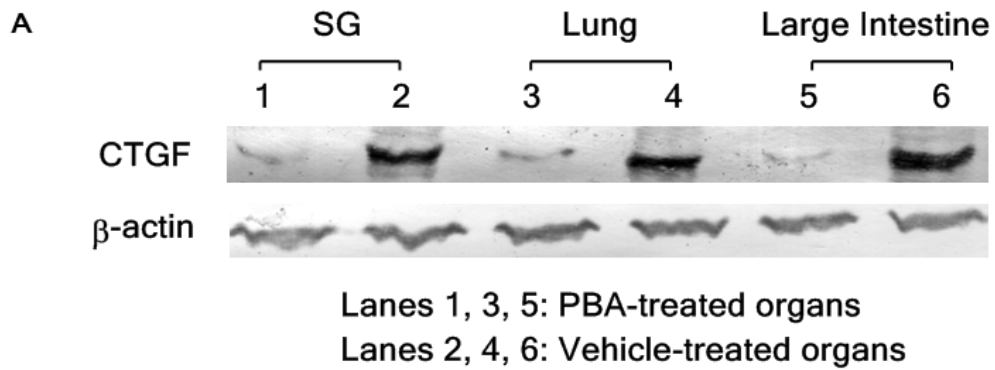
Supplementary Figure 4



184

185 **Supplementary Figure 4. Protection of intestinal and conjunctival goblet cells by the ER**
 186 **stress attenuator PBA.** (A) PAS staining for the PBA-medicated small intestine and eyes
 187 and their vehicle-medicated counterparts. Purple dots in the pictures are goblet cells. The
 188 images were taken at 200x magnification, and the scale bar is 200 μ m. (B) The density of
 189 goblet cells in the PBA-treated small intestine and eyes (blue), and their vehicle-treated
 190 counterparts (red). The values are presented as means, \pm SD, PBA: n=3, Vehicle: n=3 (small
 191 intestine), PBA: n=5, Vehicle: n=5 (eye) ***P<0.001.

Supplementary Figure 5



192

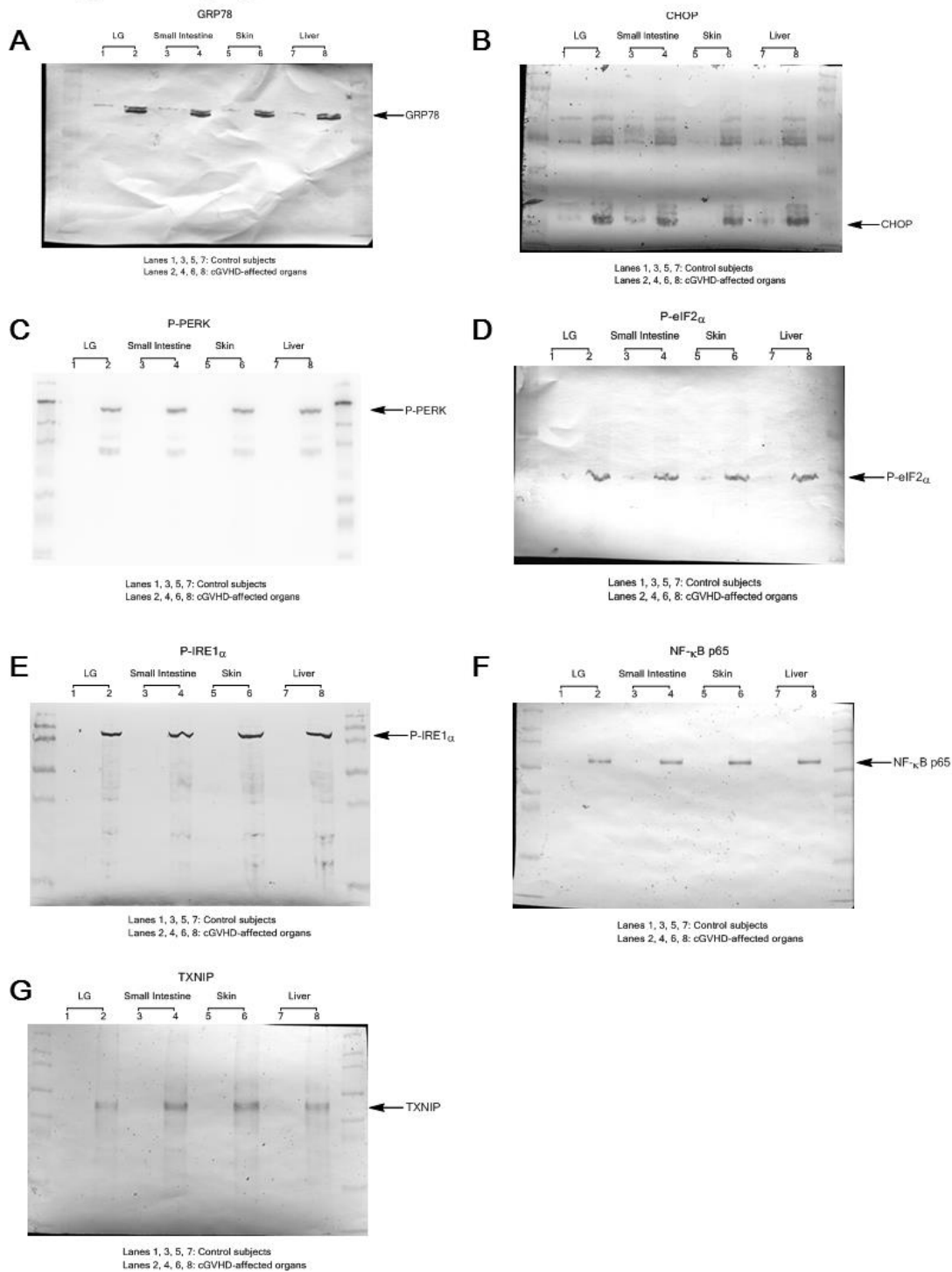
193 **Supplementary Figure 5. Reduction of fibrotic indicators utilizing the ER stress**
194 **alleviator PBA** (A) Immunoblot analysis of the fibrotic marker CTGF. (Lanes 1, 3, 5: PBA-
195 treated organs, Lanes 2, 4, 6: vehicle-treated organs) Cropped blots are displayed. (B) The
196 subsequent densitometric analysis of CTGF in each organ. PBA-treated organs (blue) and
197 vehicle-treated organs (red). Data from one of two similar experiments are shown. The data
198 are presented as means, \pm SD, PBA: n=4, Vehicle: n=4 *P<0.05.

199

200

201

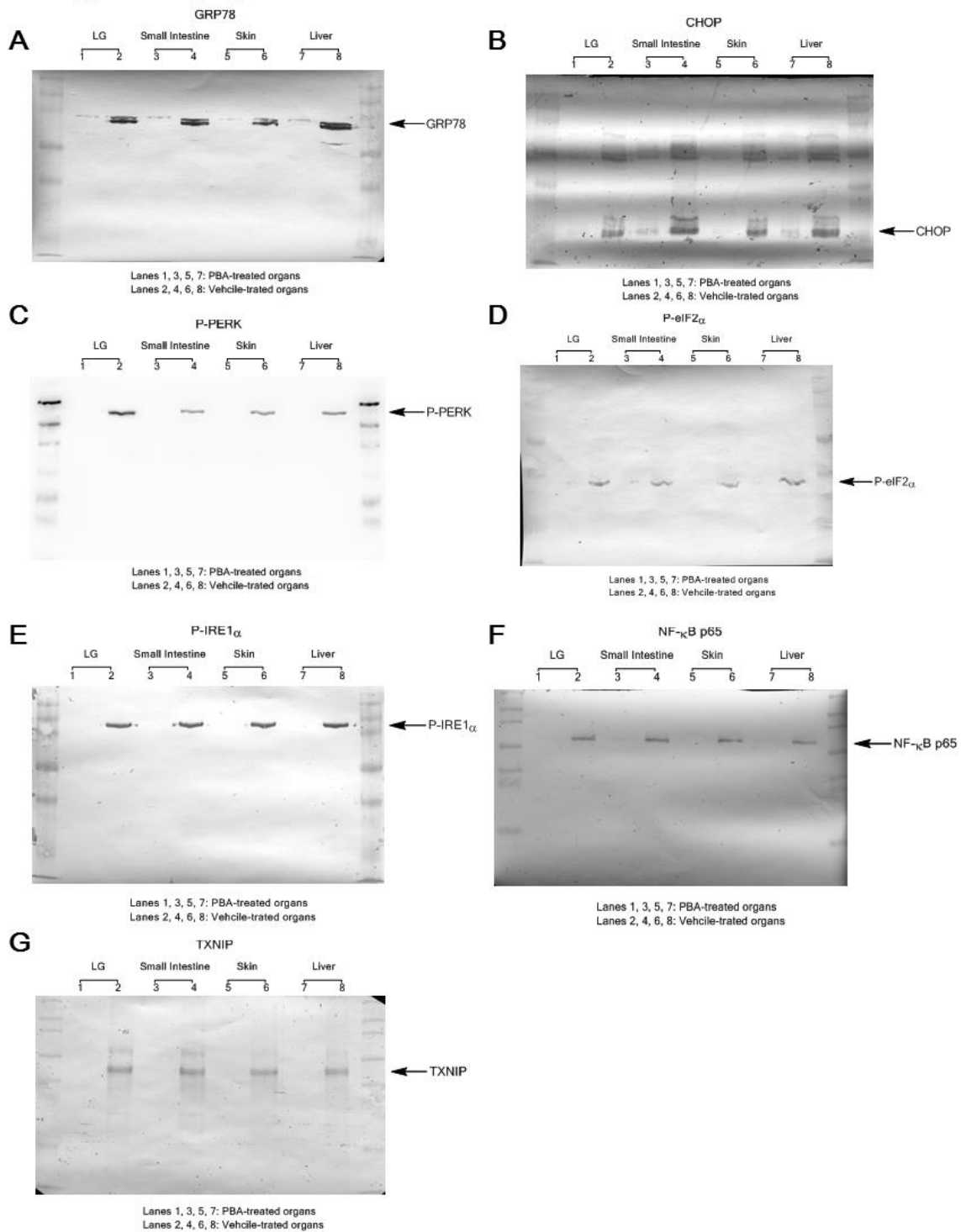
Supplementary Figure 6



202

203 **Supplementary Figure 6. Full-length gels from immunoblot assays for the ER stress**
 204 **markers and inflammation-associated molecules shown in Figure 1B.** Lanes 1, 3, 5, 7:
 205 Syngeneic control subjects, Lanes 2, 4, 6, 8: cGVHD-impaired organs. (A) GRP78, (B)
 206 CHOP, (C) P-PERK, (D) P-eIF2 α , (E) P-IRE1 α , (F) NF- κ B p65 and (G) TXNIP
 207

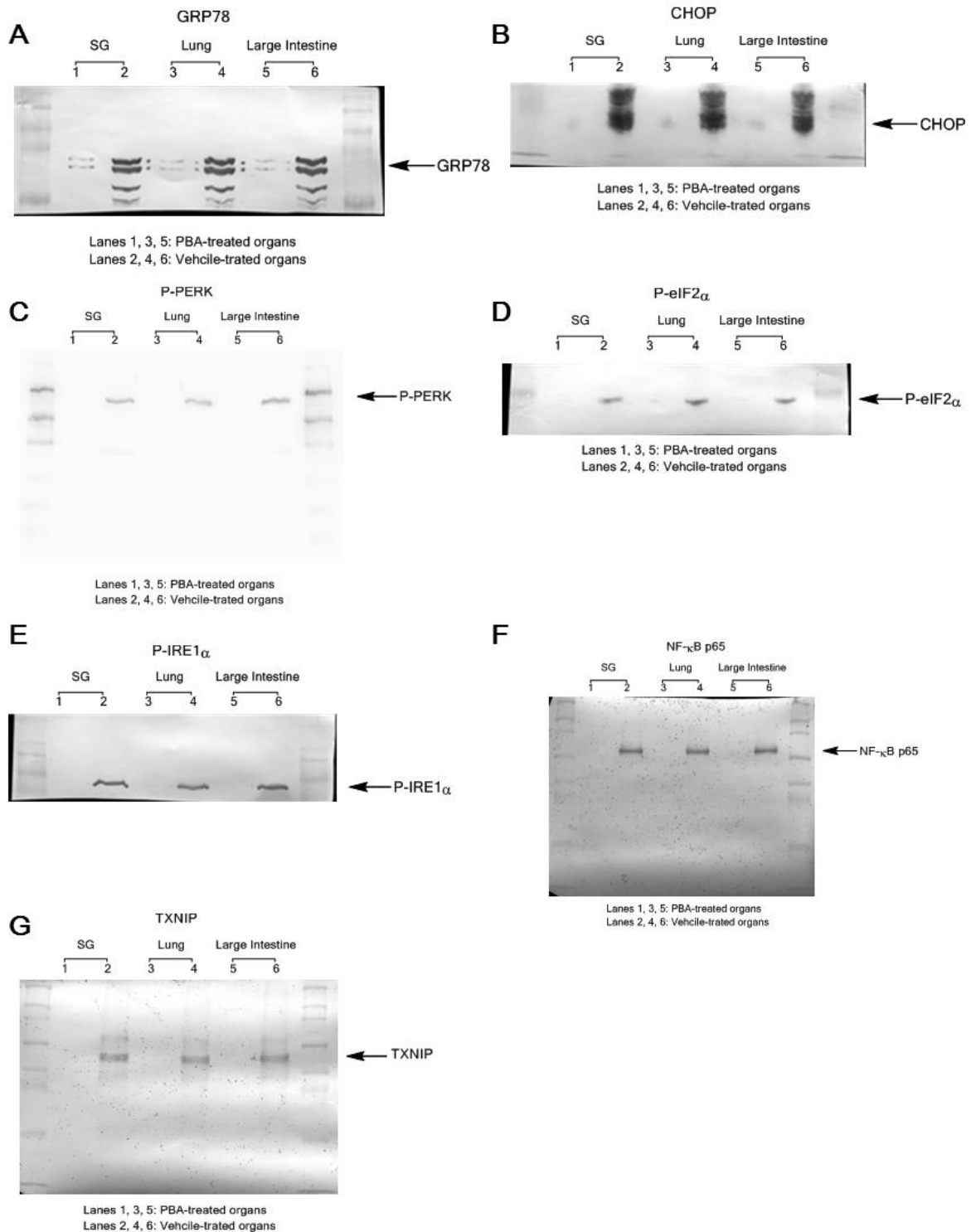
Supplementary Figure 7



208
209

210 **Supplementary Figure 7. Full-length gels from immunoblot assays for the ER stress**
 211 **markers and inflammation-associated molecules shown in Figure 2A. Lanes 1, 3, 5, 7:**
 212 **PBA-medicated organs. Lanes 2, 4, 6, 8: Vehicle-medicated organs. (A) GRP78, (B) CHOP,**
 213 **(C) P-PERK, (D) P-eIF2 α , (E) P-IRE1 α , (F) NF- κ B p65 and (G) TXNIP**

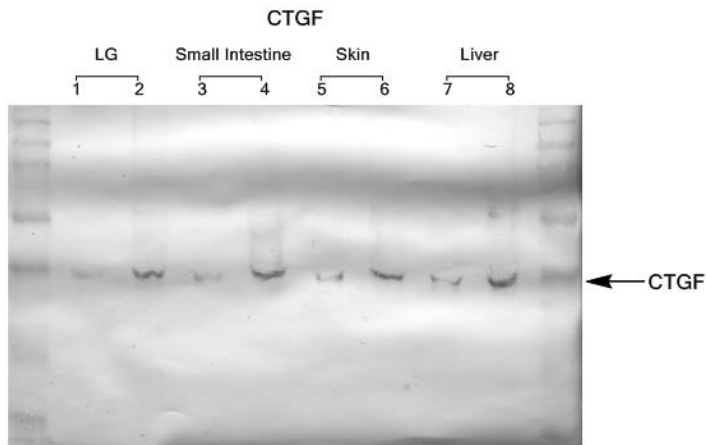
Supplementary Figure 8



214

215 **Supplementary Figure 8. Full-length gels from immunoblot assays for the ER stress**
 216 **markers and inflammation-associated molecules shown in Supplementary Figure 2A.**
 217 Lanes 1, 3, 5: PBA-medicated organs. Lanes 2, 4, 6: Vehicle-medicated organs. (A) GRP78,
 218 (B) CHOP, (C) P-PERK, (D) P-eIF2 α , (E) P-IRE1 α , (F) NF- κ B p65 and (G) TXNIP

Supplementary Figure 9



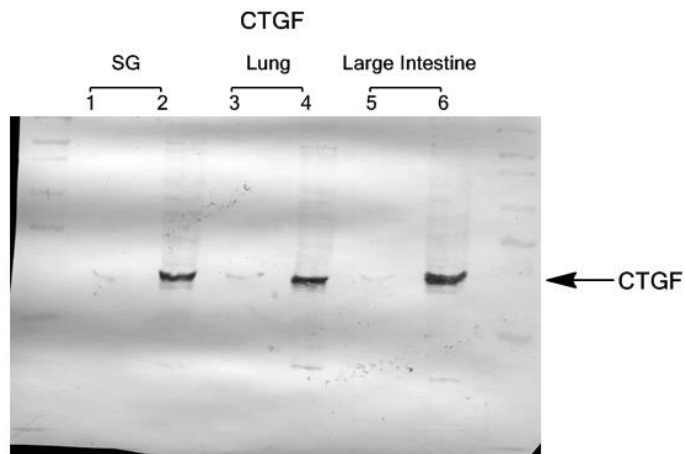
Lanes 1, 3, 5, 7: PBA-treated organs
Lanes 2, 4, 6, 8: Vehicle-treated organs

219

220 **Supplementary Figure 9. Full-length gel from immunoblot analysis of the fibrotic**
221 **marker CTGF shown in Figure 4B. Lanes 1, 3, 5, 7: PBA-medicated organs. Lanes 2, 4, 6,**
222 **8: Vehicle-medicated organs.**

223

Supplementary Figure 10



Lanes 1, 3, 5: PBA-treated organs
Lanes 2, 4, 6: Vehicle-treated organs

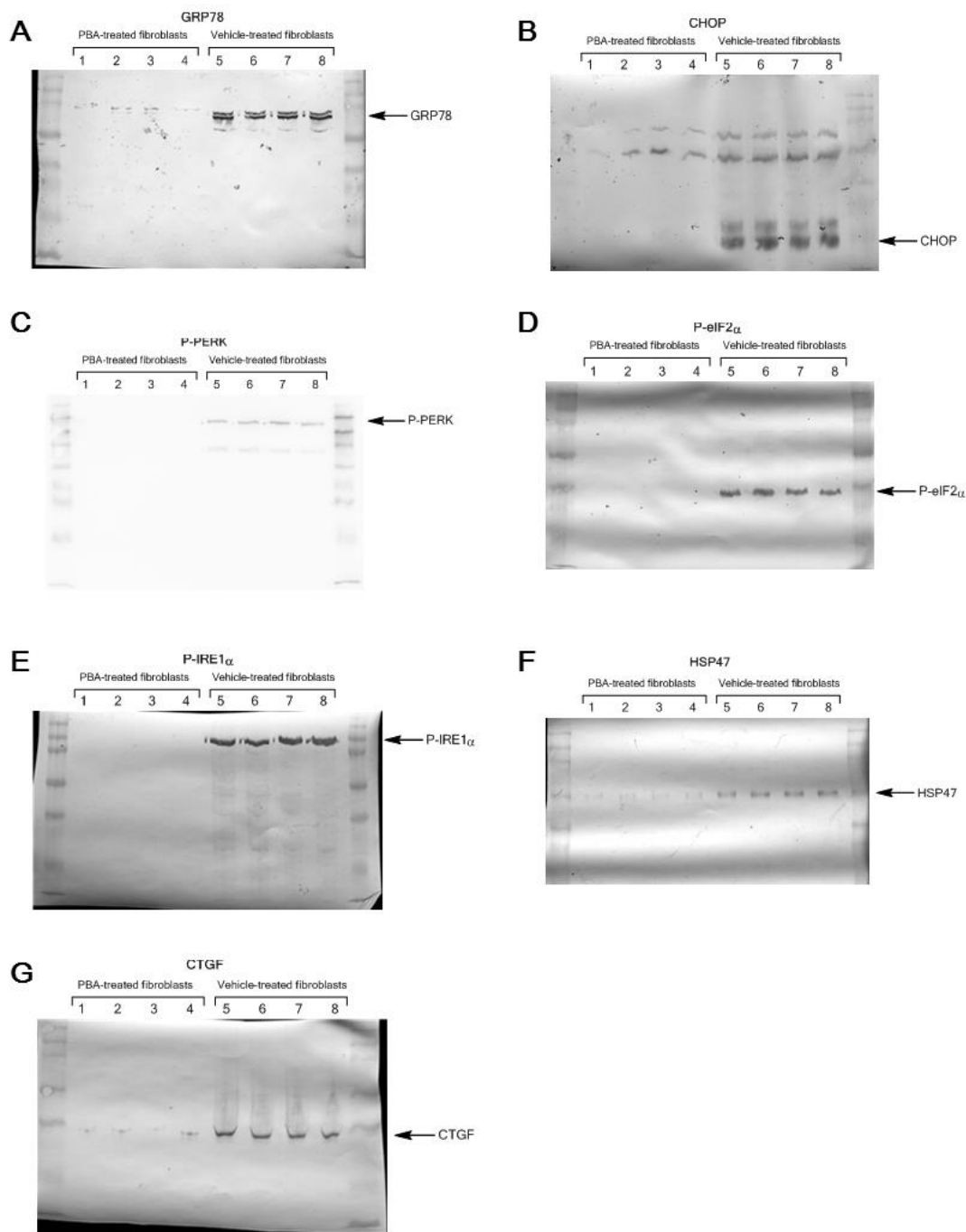
224

225 **Supplementary Figure 10. Full-length gel from immunoblot analysis of the fibrotic**
226 **marker CTGF shown in Supplementary Figure 5A. Lanes 1, 3, 5: PBA-medicated organs.**
227 **Lanes 2, 4, 6: Vehicle-medicated organs.**

228

229

Supplementary Figure 11

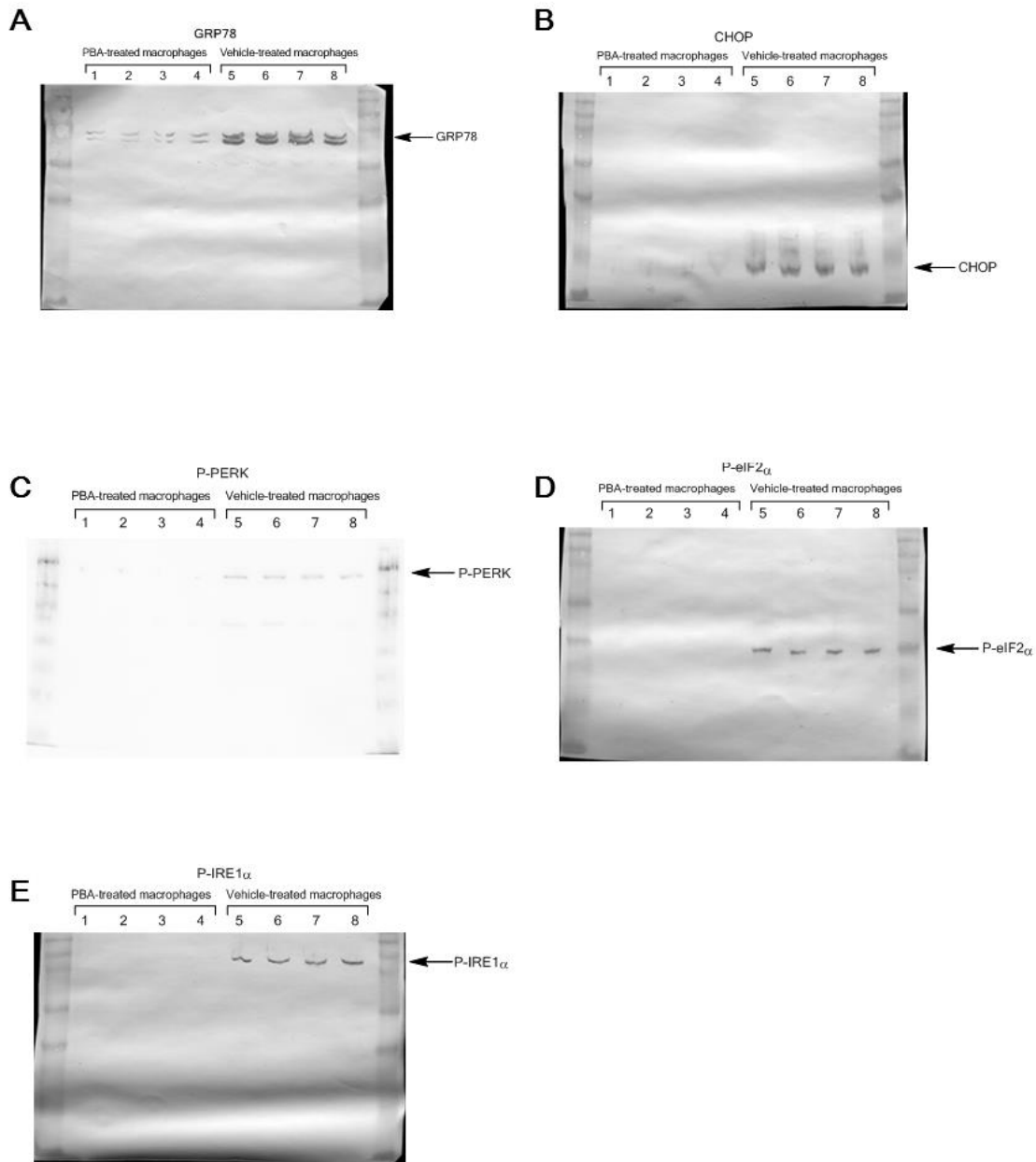


230

231 **Supplementary Figure 11. Full-length gels from immunoblot assays for the ER stress,**
 232 **activation and fibrotic markers shown in Figure 5A.** (Lanes 1, 2, 3, 4: Fibroblasts from the
 233 PBA-treated lacrimal glands, Lanes 5, 6, 7, 8: Fibroblasts from the vehicle-treated lacrimal
 234 glands). (A) GRP78, (B) CHOP, (C) P-PERK, (D) P-eIF2 α , (E) P-IRE1 α , (F) HSP47 and (G)
 235 CTGF

236

Supplementary Figure 12

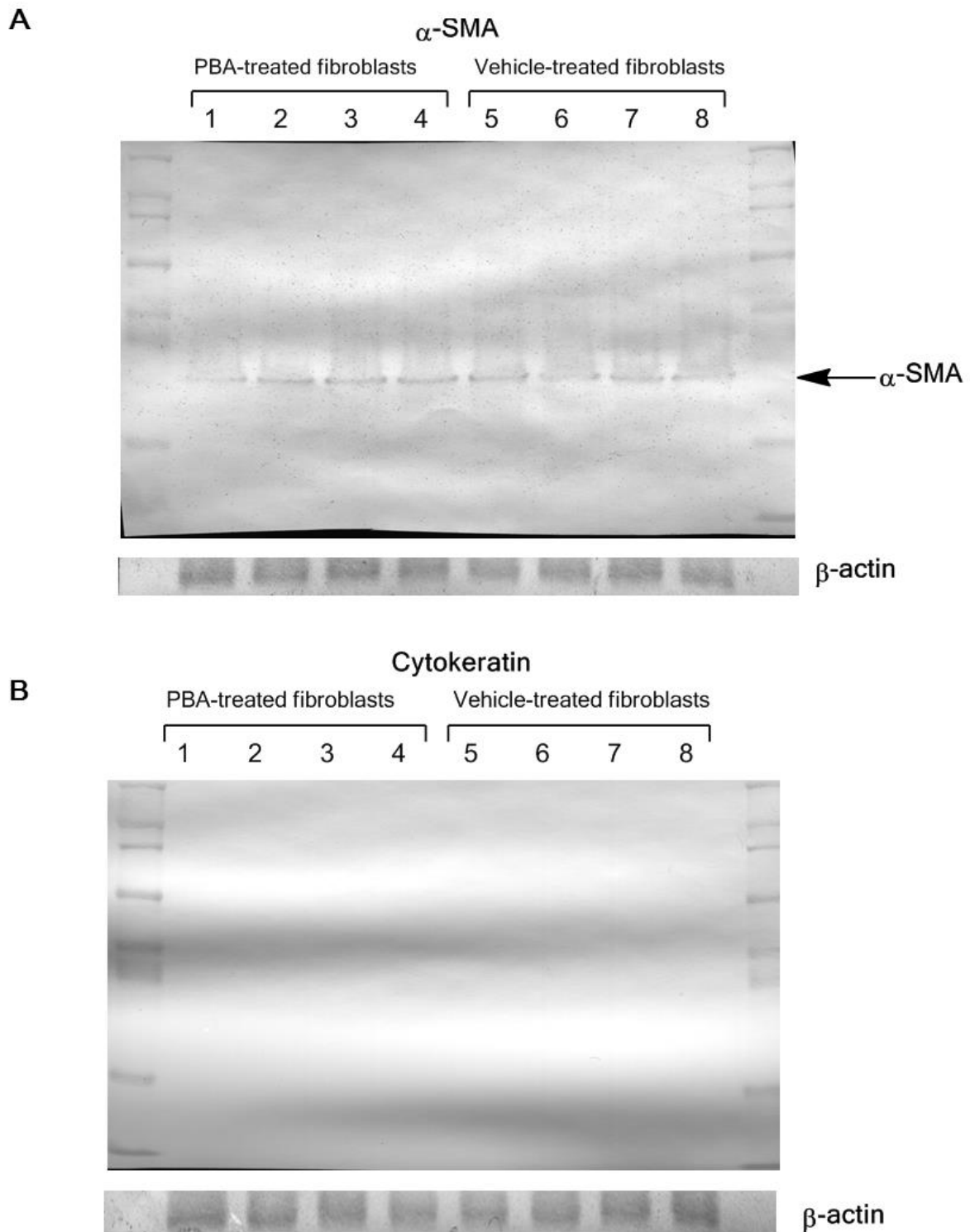


237

238 **Supplementary Figure 12. Full-length gels from immunoblot assays for the ER stress**
239 **markers shown in Figure 6C.** Lanes 1, 2, 3, 4: Splenic macrophages from PBA-dosed mice,
240 Lanes 5, 6, 7, 8: Splenic macrophages from vehicle-dosed mice). (A) GRP78, (B) CHOP, (C)
241 P-PERK, (D) P-eIF2 α , (E) P-IRE1 α

242

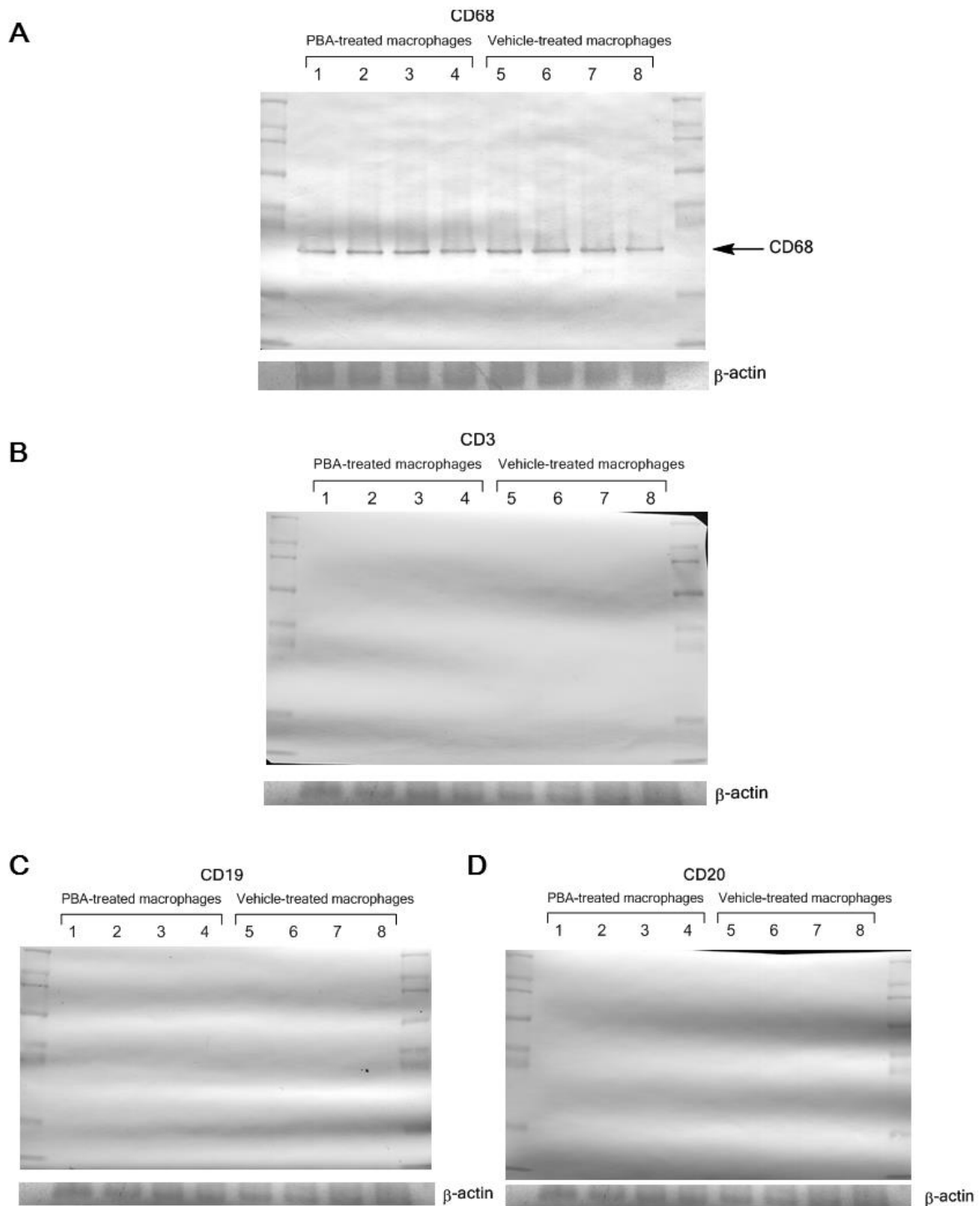
Supplementary Figure 13



243
244
245
246
247
248

Supplementary Figure 13. Full-length gels from immunoblot assays for α -SMA and cytokeratin. (Lanes 1, 2, 3, 4: Fibroblasts from the PBA-treated lacrimal glands, Lanes 5, 6, 7, 8: Fibroblasts from the vehicle-treated lacrimal glands). (A) α -SMA, (B) cytokeratin

Supplementary Figure 14



249
250
251
252
253
254

Supplementary Figure 14. Full-length gels from immunoblot assays for CD68, CD3, CD19 and CD20. Lanes 1, 2, 3, 4: Splenic macrophages from PBA-dosed mice, Lanes 5, 6, 7, 8: Splenic macrophages from vehicle-dosed mice). (A) CD68, (B) CD3, (C) CD19, (D) CD20

255 **References**

256 1. Hopwood, J. Fixation and fixtative. In: Bancroft JD, Stevens A, eds. *Theory and Practice of*
257 *Histological Techniques. 4th ed. Edinburgh: Churchill–Livingstone 23-46 (1996).*

258
259 2. Anderson, G. & Gordon, K. Tissue processing, microtomy and paraffin sections. In: Bancroft
260 JD, Stevens A, eds. T. *Theory and Practice of Histological Techniques. 4th ed. Edinburgh:*
261 *Churchill–Livingstone, 47-68 (1996).*